MOLECULAR
METABOLISM

Lack of Gα$_{i2}$ proteins in adipocytes attenuates diet-induced obesity

Check for updates

Veronika Leiss [1,9], Annika Schönsiegel [1,9], Thorsten Gnad [2], Johannes Kerner [1], Jyotsna Kaur [1], Tina Sartorius [3,4,5], Jürgen Machann [4,5,6], Fritz Schick [6], Lutz Birnbaumer [7,8], Hans-Ulrich Häring [3,4,5], Alexander Pfeifer [2], Bernd Nürnberg [1,*]

ABSTRACT

Objectives: Typically, obesity results from an inappropriate balance between energy uptake from nutrient consumption and burning of calories, which leads to a pathological increase in fat mass. Obesity is a major cause of insulin resistance and diabetes. Inhibitory G proteins (Gα$_i$) form a subfamily that is involved in the regulation of adipose tissue function. Among the three Gα$_i$ members, i.e. Gα$_{i1}$, Gα$_{i2}$, Gα$_{i3}$, the Gα$_{i2}$, protein is predominantly expressed in adipose tissue. However, the functions of the Gα$_{i2}$ isoform in adipose tissue and its impact on the development of obesity are poorly understood.

Methods: By using AdipoqCreER^{T2} mice, we generated adipocyte-specific *Gnai2*-deficient mice to study Gα$_{i2}$ function, specifically in white and brown adipocytes. These mice were fed either a control diet (CD) or a high fat diet (HFD). Mice were examined for obesity development, insulin resistance and glucose intolerance. We examined adipocyte morphology and the development of inflammation in the white adipose tissue. Finally, intracellular cAMP levels as an indicator of Gα$_i$ signaling and glycerol release as an indicator of lipolysis rates were measured to verify the impact of Gα$_{i2}$ on the signaling pathway in brown and white adipocytes.

Results: An adipocyte-specific deficiency of Gα$_{i2}$ significantly reduced diet-induced obesity, leading to decreased fat masses, smaller adipocytes and decreased inflammation in the white adipose tissue relative to littermate controls. Concurrently, oxygen consumption of brown adipocytes and *in vivo* measured energy expenditure were significantly enhanced. In addition, glucose tolerance and insulin sensitivity of HFD-fed adipocyte-specific *Gnai2*-deficient mice were improved compared to the respective controls. In the absence of Gα$_{i2}$, adrenergic stimulation of intracellular adipocyte cAMP levels was increased, which correlated with increased lipolysis and energy expenditure.

Conclusion: We conclude that adipocyte Gα$_{i2}$ is a major regulator of adipocyte lipid content in diet-induced obesity by inhibiting adipocyte lipolysis in a cAMP-dependent manner resulting in increased energy expenditure.

1. INTRODUCTION

Obesity is a rapidly expanding pandemic disorder, which associates with severe comorbidities such as metabolic syndrome, cardiovascular disease and certain types of cancer. Obesity results from an imbalance between energy intake and energy expenditure, leading to an increase in body fat mass with adipocyte hypertrophy and hyperplasia. Excessive lipid storage is associated with chronic inflammation of adipose tissue, which is considered to be a major cause of obesity-related insulin resistance and type-2 diabetes [1–4]. G-protein-coupled receptor (GPCR)-signaling represents a fundamental cellular communication paradigm and plays important roles in various organs that are involved in the control of metabolism such as the central nervous system, liver, muscle, pancreatic islets, and adipose tissue [5]. The transmembrane signal transduction from ligand-activated receptors to intracellular effector proteins is mediated *via* heterotrimeric G proteins, which consist of three subunits (Gα, Gβ and Gγ). Upon binding of a ligand to a GPCR, the associated heterotrimeric G protein is activated, leading to a dissociation of both the Gα subunit as well as the Gβγ dimer from its receptor. The G protein subunits elicit cellular responses through regulation of intracellular second messenger systems. The pertussis toxin (PTX)-sensitive Gα$_i$ family is implicated in

[1]Department of Pharmacology, Experimental Therapy and Toxicology and Interfaculty Center of Pharmacogenomics and Drug Research, University of Tübingen, 72074, Tübingen, Germany [2]Institute of Pharmacology and Toxicology, University of Bonn, 53127, Bonn, Germany [3]Department of Internal Medicine, Division of Endocrinology, Diabetology, Vascular Disease, Nephrology and Clinical Chemistry, University of Tuebingen, Tuebingen, Germany [4]German Center for Diabetes Research (DZD), Neuherberg, Germany [5]Institute for Diabetes Research and Metabolic Diseases of the Helmholtz Center Munich at the University of Tuebingen (IDM), Tuebingen, Germany [6]Section on Experimental Radiology, Department of Diagnostic and Interventional Radiology, University of Tuebingen, Germany [7]Neurobiology Laboratory, National Institute of Environmental Health Sciences, National Institutes of Health, Durham, NC, USA [8]Institute of Biomedical Research (BIOMED), Catholic University of Argentina, Buenos Aires, Argentina

[9] contributed equally.

*Corresponding author. Department of Pharmacology, Experimental Therapy and Toxicology, University of Tübingen, Wilhelmstr. 56, 72074, Tübingen, Germany. Tel.: +49 7071 29 72267. E-mail: bernd.nuernberg@uni-tuebingen.de (B. Nürnberg).

Original Article

metabolic signaling pathways to control physiological and pathophysiological conditions [1—4]. The three $G\alpha_i$ isoforms ($G\alpha_{i1}$, $G\alpha_{i2}$, $G\alpha_{i3}$), which are encoded by the genes *Gnai1*, *Gnai2*, and *Gnai3*, respectively, have been described as inhibitory $G\alpha$ subunits that suppress adenylyl cyclase activity, resulting in decreased intracellular cAMP levels [6]. The $G\alpha_i$ protein family shows a sequence homology of 85—95%. Because of this close similarity, it has been suggested that $G\alpha_i$ proteins have identical functions and play redundant physiological roles. However, recent studies in mice with global or cell-specific absence of $G\alpha_i$-isoforms highlighted their distinct biological roles [7—13]. Global *Gnai2*-deficiency results in retarded embryonic growth and reduced weight [9,12,14], defective inflammation-induced macrophage migration [12,13], and reduction in L-arginine-induced insulin secretion [9]. Although $G\alpha_{i2}$ is ubiquitously expressed, its role in cell-type specific functions, especially regarding lipid metabolism and body weight, remains to be clarified. Although all three $G\alpha_i$ isoforms are found in adipose tissue, $G\alpha_{i2}$ is the major isoform in brown (BAT) and white adipose tissue (WAT) but the specific impact and the consequences of $G\alpha_{i2}$ expression in adipocytes needs to be determined.

Here, we studied mice lacking the $G\alpha_{i2}$ protein specifically in adipocytes (*Gnai2*[ako]) by using AdipoqCreER[T2] mice. The Cre recombinase expression was under the control of the *Adiponectin* promotor and recombination had to be induced with tamoxifen injections [15]. To examine the role of $G\alpha_{i2}$ in BAT and WAT, we challenged these *Gnai2*[ako] mice with a 45% high fat diet (HFD) in comparison to their littermate controls. Lack of adipocyte $G\alpha_{i2}$ mitigated diet-induced obesity and resulted in a significant reduction of inflammatory parameters (IL-6, TNFα, crown-like structure formation), improved glucose tolerance and insulin sensitivity. *Gnai2*-deficient adipocytes in subcutaneous and visceral WAT of mice on HFD were smaller and showed reduced fat storage in these adipose tissue compartments. Lack of $G\alpha_{i2}$ in both, brown and white adipocytes caused elevated cAMP levels and lipolytic activity, which was reflected in increased energy expenditure.

These findings identify adipocyte $G\alpha_{i2}$—dependent signaling to be crucial in the development of obesity and insulin resistance. We therefore conclude that $G\alpha_{i2}$ has an isoform-specific function in brown and white adipocytes. Importantly, none of the remaining $G\alpha_i$ isoforms compensated for the missing $G\alpha_{i2}$. In fact, $G\alpha_{i2}$-deficiency increased lipolytic activity of brown and white adipocytes in a cAMP-dependent manner, which is likely to explain an increased energy expenditure and a significantly reduced weight gain under high caloric conditions.

2. METHODS

2.1. Animals and diets
To obtain a tissue-specific deletion of $G\alpha_{i2}$ in adipocytes (*Gnai2*[ako]), mice on a C57BL/6N background, carrying a tamoxifen-inducible adipose tissue-specific Cre recombinase under the control of the adiponectin promoter (genotype *adiponectin*-CreERT2[+/tg]), were mated to homozygous animals of the floxed *Gnai2* mouse line (genotype *Gnai2*^{fl/fl}) [7,9,15].

Genotyping was performed using specific primers to identify the Cre transgenes as well as the floxed and wild-type alleles of *Gnai2* on DNA samples obtained from ear or tail-tip biopsies. Premutant animals (genotype *Gnai2*^{fl/fl}; *adiponectin*-CreERT2[+/tg]) and their littermate controls (ctrl; genotype *Gnai2*^{fl/fl}) derived from the respective breeding were injected with tamoxifen (1 mg/day) for 5 consecutive days at an age of 4 weeks to induce Cre-mediated recombination [15,16]. Before administering the different research diets, all experimental mice received a commercial standard chow (SNIFF). Starting at the age of 6

weeks, dietary feeding trials were performed in male mice that received either a defined control diet (CD) formulation containing 10% of calories from fat or a high-fat diet (HFD) containing 45% of calories from fat (both obtained from Research Diets, New Brunswick, NJ, USA) for another 22 weeks. Progressive body weight gain was monitored weekly. During the studies, animals had free access to drinking water. All animal experiments were approved by the local government's Committee on Animal Care and Welfare and conducted in accordance with the German legislation on the protection of animals. All mice analyzed within this study were bred and maintained in the animal facility of the Institute of Experimental and Clinical Pharmacology and Pharmacogenomics, Eberhard Karls University, Tübingen. They were housed in individually ventilated cages (IVC) under specific-pathogen-free conditions with temperatures maintained between 21 °C and 24 °C, humidity at 45—55% and a 12-h light/dark cycle. All experimental protocols were based on the institutional guidelines of the Veterinary Care Unit, University of Tübingen and Bonn and were approved by the animal welfare commissioner of the regional board for scientific animal experiments in Tübingen and Bonn. Experiments were performed according to the European Union Directive 86/609/EEC for the protection of animals used for experimental and other scientific purposes.

2.2. Food and water intake
For measurement of food and water intake, mice were housed individually. Food consumption was assessed on four consecutive days. The amount of food and water consumed by each individual mouse was determined by calculating the weight differences between the initial weight of the food pellets or water bottle and the final weight 24 h later.

2.3. Bomb calorimetry
Energy excreted in feces was measured using a bomb calorimeter (Parr Instrument Company model 6725).

2.4. Magnetic resonance imaging
For quantification of fat volume, magnetic resonance imaging (MRI) studies were performed on a 3 T whole-body imager (Magnetom Trio, Siemens Healthcare, Erlangen, Germany). Mice were anaesthetized with ketamine (2 mg)/xylazine (0.4%) and were positioned in prone position in the wrist coil of the manufacturer and MRI examinations were simultaneously performed in *Gnai2*[ako] mice and their respective control (ctrl) littermates. An in-plane spatial resolution of 0.4 mm and a slice thickness of 2 mm allowed recording of abdominal fat images. The fat volume was calculated as described in [17,18].

2.5. Time-domain-nuclear magnetic resonance analysis
Fat mass, lean mass and extracellular fluid were analyzed using time-domain-nuclear magnetic resonance analysis (TD-NMR; LF50; Bruker, Massachusetts, USA) in mice.

2.6. Energy expenditure
Energy expenditure was measured individually over 24 h with Phenomaster/TSE Systems (Bad Homburg, Germany). Mice were allowed to acclimate to metabolic chambers for 24 h before measurements.

2.7. Adipose tissue mass
To determine masses of different fat depots, all pads of brown adipose tissue (BAT), gonadal white adipose tissue (gWAT) and inguinal white adipose tissue (iWAT) were dissected, weighed as a whole, before being cut into smaller pieces, immersed in liquid nitrogen and finally stored at −80 °C for further analysis.

2.8. PCR analysis

PCR amplification was performed with specific primers to identify the Cre transgene, the floxed and the wild-type allele of *Gnai2*, after extraction of DNA from different tissues of *Gnai2*[ako] mice, as well as adipocytes of various other genotypes using a lysis buffer containing proteinase K.

DNA samples were separated by size *via* agarose gel electrophoresis using a 2% agarose gel stained with ethidium bromide.

2.9. RNA isolation and qPCR

Total RNA was isolated from tissues using TRIzol (peqLab). Reverse transcription was performed using Transcriptor First Strand Synthesis Kit (Roche). qPCR was performed using SYBR-Green (Roche) and a Light Cycler 480 instrument (Roche). Fold changes were calculated using relative quantification methods with β-actin serving as internal control.

2.10. Immunoblot analysis

Dissected BAT, gWAT and iWAT pads were homogenized in lysis buffer containing 100 mM NaCl, 20 mM Tris—HCl, 2.5 mM EDTA and protease inhibitors (Complete Roche; Roche, Mannheim, Germany) to generate total protein lysates for subsequent immunoblot analyses. The proteins were precipitated with a 3:1 ratio of methanol to chloroform prior to separation by molecular weight *via* 12% SDS gels containing 6 M urea to achieve proper electrophoretic separation of Gα$_i$ isoforms, and subsequently transferred onto polyvinylidene difluoride membranes (PVDF; Merck Millipore, Darmstadt, Germany). The membranes were blocked in 5% milk—TBST (tris-buffered saline (TBS)—Tween 20), incubated with the indicated antibodies and developed with enhanced chemiluminescence (ECL; GE Healthcare, Buckinghamshire, UK).

For immunodetection of Gα$_{i1}$ and Gα$_{i2}$ proteins, the following primary antibody was used directed against the very last 21 amino acids of the C-terminus: rabbit anti-Gα$_{i1/i2}$ (1:5000) [9,14,19,20]. Loading controls were performed with antibodies against mouse anti-β-actin (1:5000; Sigma—Aldrich, Taufkirchen, Germany). As secondary antibodies, anti-rabbit HRP (1:2000; Cell Signaling Technology, Danvers, MA, USA) and anti-mouse HRP (1:2000; Dako, Glostrup, Denmark) were applied. The protein levels of Gα$_{i1}$ and Gα$_{i2}$ were quantified using densitometric analysis software (Image Lab; Bio-Rad, Hercules, CA, USA) and normalized to the β-actin levels of the same samples.

The analyses were run in three independent experiments for each animal analyzed. The mean values for the single probes were built and overall mean was calculated.

2.11. Glucose and insulin tolerance test

For the glucose tolerance test, mice were fasted overnight. Blood glucose levels were determined using a Contour® XT glucometer (Bayer, Leverkusen, Germany) immediately before an intraperitoneal (i.p.) injection of glucose (2 mg/g body weight) and 15, 30, 60 and 120 min after the injection. At each time point, additional blood samples were collected *via* the tail vein for subsequent insulin determination.

For the insulin tolerance test, mice were fasted for 4 h, followed by an i.p. injection of insulin (1 mU/g body weight). 1.5 μM aprotinin was added to the blood samples. Blood glucose levels were measured before the injection and 15, 30, 60 and 120 min after using a Contour® XT glucometer (Bayer, Leverkusen, Germany).

2.12. Blood parameters

Plasma levels of insulin were measured using a commercially available insulin ELISA method (Mercodia, Uppsala, Sweden). Leptin, resistin,

interleukin 10 (IL-10) and tumor necrosis factor alpha (TNFα) concentrations were measured in plasma samples using Bio-Rad Bio-Plex® Multiplex Immunoassays (Bio-Rad, Hercules, USA), according to the manufacturer's instructions.

2.13. Adipose tissue histology

To quantify adipocyte area, fat pads were isolated and fixed in 4% paraformaldehyde for 24 h. Samples were dehydrated through graded ethanol and embedded in paraffin. Serial 6 μm thick sections of gWAT and iWAT were prepared and stained with hematoxylin and eosin (H&E). Images (20× magnification) were acquired using the Zeiss Axio Imager M2 microscope (Carl Zeiss, Jena, Germany). Adipocyte area was measured from digital images with the AxioVision software version 4.8 (Carl Zeiss, Jena, Germany).

For F4/80 immunohistochemistry, slices were deparaffinized and rehydrated. Antigen retrieval was performed by boiling samples in citrate buffer pH 6 (0.1 M citric acid and 0.1 M sodium citrate). Sections were treated with 3% hydrogen peroxide and then incubated in 5% normal goat serum in PBS (blocking solution). After overnight incubation at 4 °C with the primary antibody (rat-anti-mouse F4/80; 1:500; Bio-Rad) and subsequent incubation with an anti-rat-biotinylated secondary antibody (1:500; Dako) for 30 min at room temperature, detection was performed using avidin-biotin complex (Vectastain Elite ABC Kit; Vector Laboratories, Burlingame, CA, USA) and 0.05% 3,3′-diaminobenzidine (DAB). For quantification of crown like structures (CLS), adipocytes and the number of CLS were counted in at least three different sections for every animal using the AxioVision software.

2.14. Oil Red O staining

Livers were fixed in PBS containing 4% paraformaldehyde. After washing with PBS, liver slices were incubated with Oil Red O (Sigma—Aldrich, St. Louis, USA) solution (3 mg/ml in 60% isopropyl alcohol) for 15 min at room temperature, washed with PBS, and visualized under the microscope.

2.15. Lipolysis and cAMP measurements

Fat pads were harvested and cut into small pieces, which were weighed and incubated in 600 μl of lipolysis medium (Gibco® DMEM 21063, Thermo Fisher Scientific, Waltham, MA, USA; supplemented with 2% BSA) either without additive or 10 μM isoproterenol. After 1 h of incubation at 37 °C, medium was collected, followed by determination of the glycerol concentration using a free glycerol assay kit (Abcam, Cambridge, UK), according to the manufacturer's instructions. Sample absorbance was measured at 570 nm using the Tecan Sunrise microplate reader (Tecan, Männedorf, Switzerland). Glycerol content was normalized to the initial tissue weight.

For cAMP measurement, fat pads were treated in an analogous manner and incubated in medium additionally supplemented with 1 mM 3-isobutyl-1-methylxanthine (IBMX) and containing the respective additives for 15 min. Adipose tissue pieces were collected after incubation and frozen in liquid nitrogen. Subsequently, the intracellular content of cAMP was detected with a cAMP competitive enzyme immunoassay (R&D Systems, Minneapolis, MN, USA), according to the manufacturer's instructions.

2.16. Seahorse assay

To measure oxygen consumption rate (OCR), an indicator of mitochondrial respiration, we used the state-of-the-art Seahorse Extracellular Flux (XF) 96 Analyzer (Seahorse Bioscience, North Billerica,

MA, USA). Basal respiration, norepinephrine-induced respiration, ATP-linked respiration, proton leak respiration and reserve capacity were determined for each parameter in three repeated rates over a 20 min period. Baseline cellular oxygen consumption was measured by subtracting non-mitochondrial respiration.

2.17. Triglyceride content
To determine triglyceride content in liver, gWAT and iWAT the tissue was homogenized in ddH_2O supplemented with 5% NP-40. The samples were heated to 80 °C for 5 min, cooled down to room temperature and TG content was measured according to the manufacturer's instructions (Abcam, Cambridge, UK). TG content in the plasma was directly measured.

2.18. Non-esterified fatty acid content
To determine plasma NEFA levels, mice were fasted for 12 h and blood samples were taken. The NEFA content was measured with a free fatty acid quantification kit according to the manufacturer's instructions (Sigma—Aldrich, St. Louis, USA).

2.19. Il-6 content
Dissected gWAT and iWAT pads were homogenized in lysis buffer containing 100 mM NaCl, 20 mM Tris—HCl, 2.5 mM EDTA and protease inhibitors (Complete Roche; Roche, Mannheim, Germany). Blood samples were collected via the tail vein for subsequent plasma extraction as recommended by the manufacturer's instructions. IL-6 contents were measured according to the manufacturer's instructions (R&D Systems, Minneapolis, MN, USA).

2.20. Statistical analysis
All data are presented as mean ± SEM. Statistical analysis was performed using a two-tailed Student's t-test for unpaired comparison or two-way analysis of variance (ANOVA) with the post hoc Bonferroni test for multiple comparisons, where appropriate. Total energy expenditure was analyzed using analysis of covariance (ANCOVA).

For all tests, $p < 0.05$ was considered significant (*), $p < 0.01$ was considered very significant (**) and $p < 0.001$ was considered extremely significant (***).

3. RESULTS

3.1. Characterization of adipocyte-specific *Gnai2*-deficient mice
The inducible adipocyte-specific *Gnai2*-deficient mouse line was termed *Gnai2*ako (genotype: *Gnai2*fl/fl; *Adipoq*CreER$^{T2+/tg}$). By crossing *Adipoq*CreER$^{T2+/tg}$ mice [15] with mice carrying floxed *Gnai2* alleles [21], the expected genotypes were achieved. The different genotypes were born at expected Mendelian ratios and were viable and fertile. To induce recombination, the ligand-dependent chimeric CreER recombinase was activated with intraperitoneal application of tamoxifen to recombine and excise the floxed *Gnai2* DNA sequence, specifically in adipocytes. Recombination was confirmed by genomic PCR analysis (Supplemental Figs. 1A and B). DNA isolated from tails and adipocytes of tamoxifen-injected ctrl (*Gnai2*+/+; adipoqCreER$^{T2+/tg}$; *Gnai2*fl/fl; *Gnai2*+/+; *Gnai2*+/fl) animals as well as biopsies derived from the brain, liver, pancreas, and tails of tamoxifen-injected *Gnai2*ako mice remained unaffected by CreER activity (Supplemental Fig. 1B). In contrast, recombination was solely detectable in gonadal (gWAT; visceral adipose tissue) and inguinal white adipose tissue (iWAT; subcutaneous adipose tissue), and, most importantly, in DNA from partially purified adipocytes from *Gnai2*ako mice indicated by the additional 390 bp band (Supplemental Fig. 1B). To verify

recombination at the protein level in the *Gnai2*ako mice, immunoblot analyses were performed to study the expression pattern of the Gα$_{i2}$ protein in liver, skeletal muscle, brain, BAT, gWAT, iWAT and primary white adipocytes (WA). Using specific antibodies against the identical COOH-terminal sequence of the Gα$_{i1}$ and Gα$_{i2}$ protein, both isoforms were detectable in gWAT, iWAT and primary white adipocytes derived from control and wildtype animals (Figure 1A). Interestingly, BAT only expresses the Gα$_{i2}$ protein (Figure 1A). Consistent with our adipocyte-specific mouse model, the Gα$_{i1}$ protein (upper band) was also detectable in adipose tissue lysates derived from *Gnai2*ako and global *Gnai2*-deficient mice but absent in *Gnai1*-deficient mice. Importantly, its expression level was not affected by the Cre recombination in *Gnai2*ako adipose tissue homogenates and primary white adipocytes (Supplemental Figs. 1C—E). Consistent with a cell type-specific deletion Gα$_{i2}$ expression levels in liver, skeletal muscle and brain were not affected by the Cre-driven recombination in adipocytes (Supplemental Figs. 1F and G). In contrast, the Gα$_{i2}$ protein (lower band) showed a significant reduction in gWAT, iWAT and BAT of *Gnai2*ako mice (Supplemental Figs. 1H—J) and was completely absent in global *Gnai2*-deficient adipose tissue lysates (Figure 1A). We consider most of the remaining Gα$_{i2}$ immunoreactivity in *Gnai2*ako in gWAT, iWAT and BAT likely results from the expression of Gα$_{i2}$ in non-adipose cells like vessels or connective tissue since analysis of Gα$_{i2}$ protein levels in primary white adipocytes revealed an 80% reduction compared to control adipocytes (Supplemental Fig. 1K). Of note, Gα$_{i1}$ expression levels were not altered in *Gnai2*ako mice, regardless of the diet fed arguing against any compensatory mechanisms of Gα$_{i1}$ for Gα$_{i2}$. Hence, the adipocyte-specific knockout model for *Gnai2* should allow us to test the role of adipocyte Gα$_{i2}$ for body weight gain and energy expenditure under different dietary conditions focusing on fat cell function.

3.2. Body composition of adipocyte-specific *Gnai2*-deficient mice
To study the consequences of adipocyte-specific Gα$_{i2}$ ablation on the metabolic homeostasis, body weight gain was recorded in adipocyte-specific *Gnai2*-deficient and age- and litter-matched control mice, receiving either a purified, low-fat control diet (CD) or a high fat diet (HFD) with 45% of its calories derived from lipids. Animals were allowed to recover from the tamoxifen-injections for one week before they were subjected to the distinct diets. Before onset of the dietary program, no differences in size or body weight were observed between the *Gnai2*ako and ctrl mice (Figure 1C). Subsequently, mice deficient for Gα$_{i2}$, specifically in adipocytes, gained markedly less weight following a HFD-challenge compared to controls (Figure 1B—D). The difference reached statistical significance after 6 weeks on HFD (12 weeks of age) and maintained significant until the end of the study (22 weeks of age). In contrast, mice kept under CD conditions gained much less weight, and none of the parameters studied differed between ctrl and *Gnai2*ako mice (Figures 1-5; Supplemental Figs. 4 and 5).

Obesity is defined by the excess storage of fat mass. To confirm that total body fat mass was altered in HFD-fed *Gnai2*ako compared to ctrl mice, we used magnetic resonance imaging (MRI) and time domain-nuclear magnetic resonance (TD-NMR) approaches. HFD-fed *Gnai2*ako mice displayed significantly less total fat mass compared to ctrl mice (Figure 1E—G). In addition, the amount of visceral body fat mass was significantly reduced at 22 weeks of age (Figure 1E,F). Importantly, lean mass and the amount of extracellular fluid were similar in *Gnai2*ako and ctrl animals (Figure 1G). In addition, neither stool caloric content measured by bomb calorimetry, food and water intake nor physical activity differed between HFD-fed ctrl and *Gnai2*ako mice (Supplemental Fig. 2B, Figure 1H—J). To corroborate our MRI and
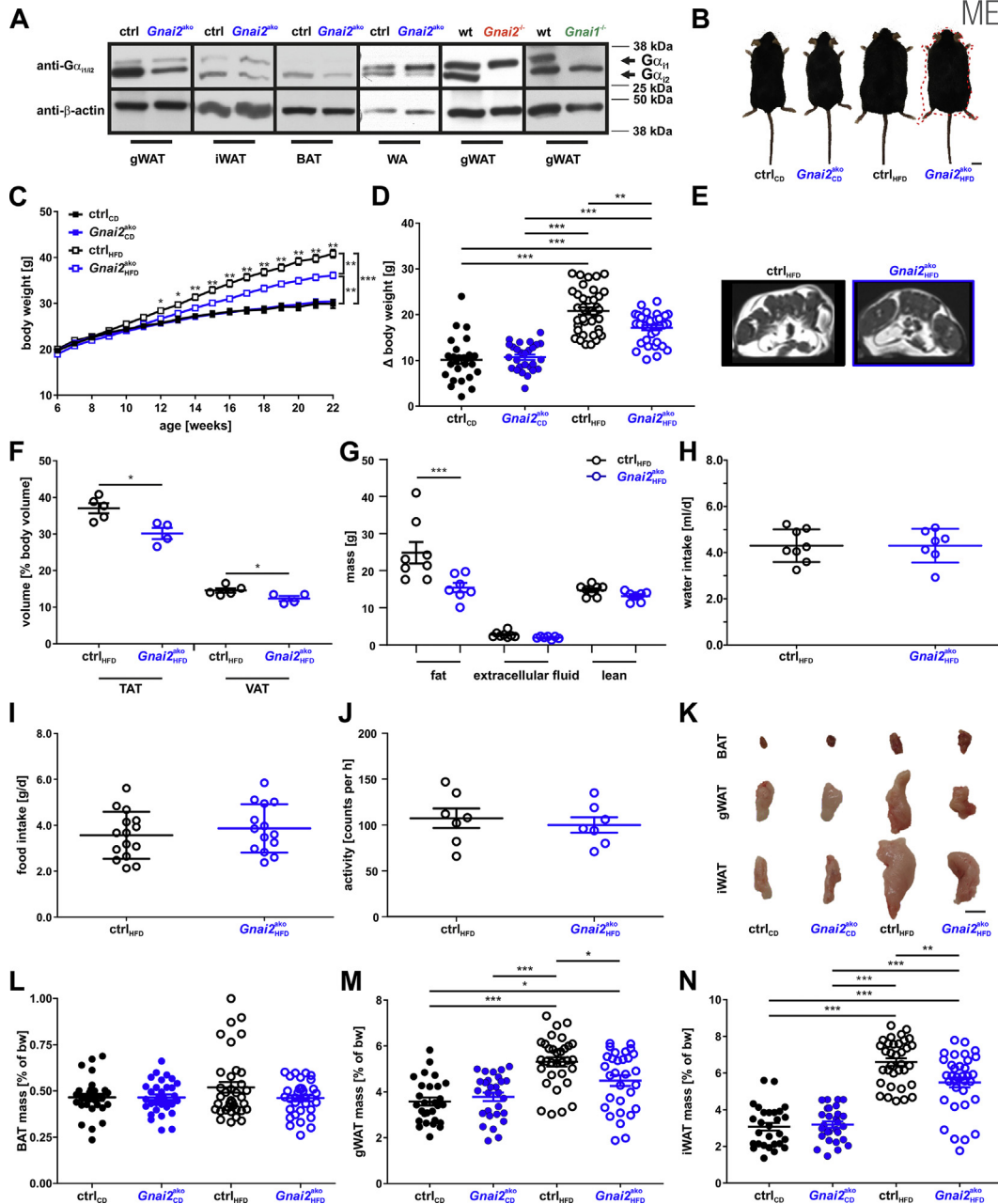
Figure 1: Reduced body weight gain in *Gnai2*^ako mice receiving 45% HFD. (A) Representative immunoblots of gonadal (gWAT), inguinal white adipose tissue (iWAT), brown adipose tissue (BAT) and primary white adipocyte (WA) homogenates isolated from ctrl, *Gnai2*^ako, wild-type (wt), global *Gnai2*- (*Gnai2*^−/−), and *Gnai1*- (Gnai1 ^−/−) deficient mice. The Gα_{i2} protein is reduced in WAT, BAT and WA of *Gnai2*^ako and completely absent in *Gnai2*^−/− white adipose tissue. The top band indicates Gα_{i1} expression since the antibody is directed against the last 14 C-terminal amino acids, which are 100% identical in the Gα_{i1} and Gα_{i2} amino acid sequence. As a control WAT homogenates derived from *Gnai1*^−/− mice were loaded. Equal loading was confirmed by β-actin detection. 20 μg protein were loaded in each lane. (B) Representative images from CD- and HFD-fed ctrl and *Gnai2*^ako mice after 22 weeks of dietary feeding. The red-dotted line indicates the silhouette of the HFD-fed control mouse. Scale bar = 1 cm (C) Body weight development under CD feeding (n = 30 per genotype per time point) and HFD feeding of ctrl (n = 38) and adipocyte-specific *Gnai2*-deficient mice (n = 35). Body weight curves of *Gnai2*^ako mice on HFD were significantly lower compared to HFD-fed ctrl mice. Lack of Gα_{i2} in adipocytes did not affect body weight gain of CD-fed *Gnai2*^ako mice in comparison to CD-fed ctrl mice. (D) Difference (Δbw) between the initial body weight (at week 6) and the final body weight (at week 22) in *Gnai2*^ako and ctrl mice under CD- and HFD-feeding conditions (n = 27 per genotype for CD; ctrl n = 38; *Gnai2*^ako n = 35 for HFD). (E) Magnetic resonance images of cross-sections of HFD-fed ctrl and *Gnai2*^ako mice after 16 weeks of HFD feeding (Bright (hyperintense) areas indicate fat tissue). (F) Calculated volumes of total adipose tissue integrated over 24 slices derived during magnetic resonance imaging were quantified of n = 5 (ctrl) and n = 4 (*Gnai2*^ako) per group on HFD. TAT — total adipose tissue; VAT — visceral adipose tissue. (G) Time domain-nuclear magnetic resonance analysis revealed significantly reduced fat masses, but similar extracellular fluid and lean mass of HFD-fed *Gnai2*^ako mice relative to controls. Water (H), food intake (I) and physical activity (J) were similar in HFD-fed ctrl and *Gnai2*^ako mice. (K) Representative images of selected BAT, gWAT and iWAT fat depots of CD- or HFD-fed ctrl and *Gnai2*^ako mice. Scale bar = 1 cm. Mass of BAT (L), gWAT (M) and iWAT (N) depots of ctrl and *Gnai2*^ako mice receiving either a CD or HFD (ctrl_CD n = 28; *Gnai2*^ako_HFD n = 28; ctrl_HFD n = 34; *Gnai2*^ako_HFD n = 34). Data were analyzed using multiple comparison two-way ANOVA followed by post-hoc comparison with Bonferroni's multiple comparison (C, D, F, G, L-N) or the Student t test (H-J) and are presented as means ± SEMs. Statistical difference between the two genotypes is indicated: *$P < 0.05$, **$P < 0.01$, ***$P < 0.001$.
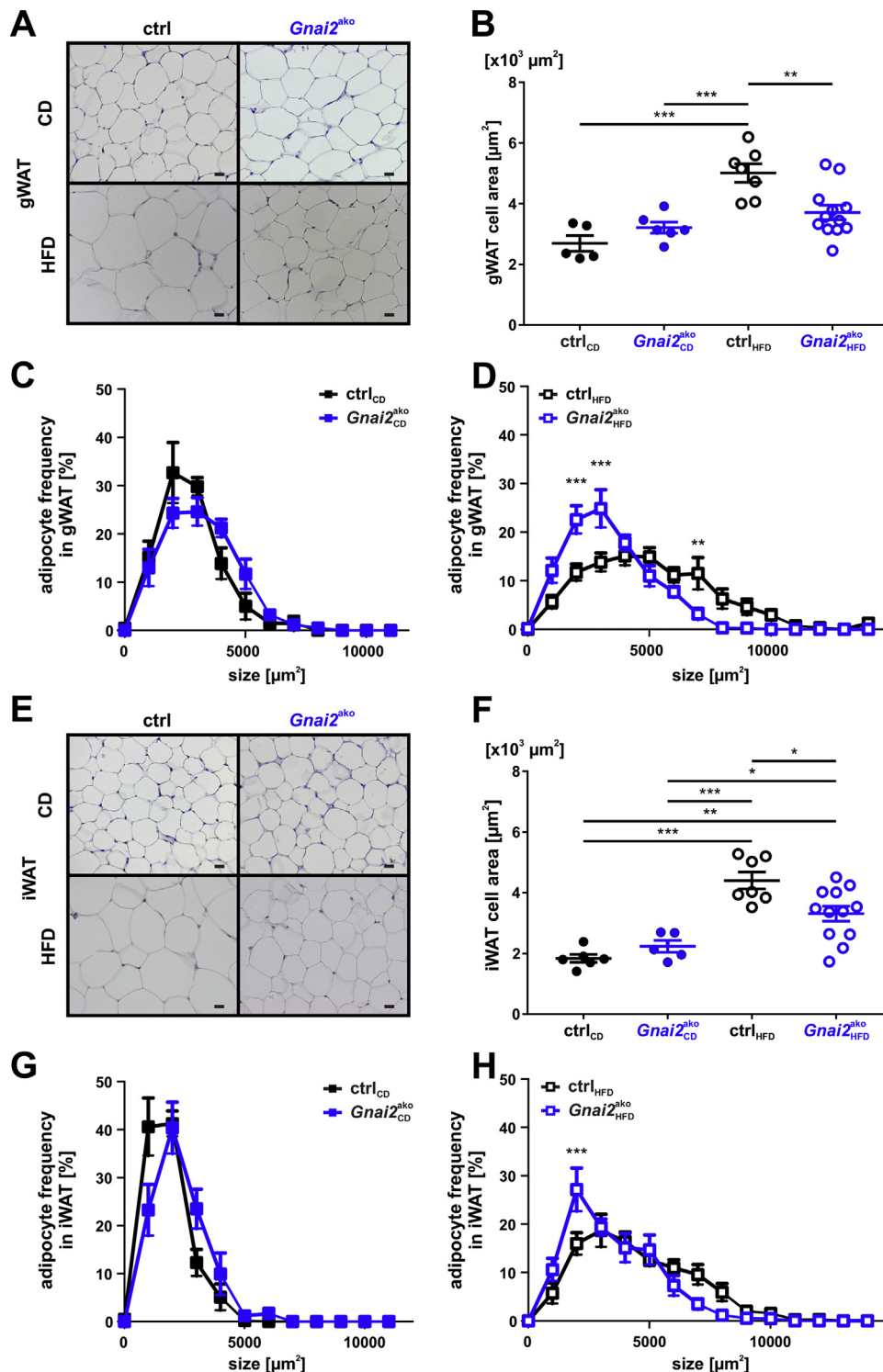
Figure 2: Reduced fat cell size in HFD-fed *Gnai2*ako mice. *(A)* Representative paraffin sections of gWAT derived from 28-week-old CD- (upper panel) or HFD-fed (lower panel) ctrl and *Gnai2*ako animals. Scale bar = 20 μm. *(B)* Average cell size of gWAT adipocytes after 22 weeks of CD or HFD feeding was analyzed in paraffin-embedded serial sections by measuring the circumference of the adipocytes. Adipocytes were significantly smaller in HFD-fed *Gnai2*ako mice. Adipocyte size distribution in gWAT of mice fed either *(C)* CD or *(D)* HFD (ctrl$_{CD}$ n = 5; *Gnai2*ako$_{HFD}$ n = 6; ctrl$_{HFD}$ n = 7; *Gnai2*ako$_{HFD}$ n = 11). *(E)* Representative paraffin sections of iWAT derived from 28-week-old CD- (upper panel) or HFD-fed (lower panel) ctrl and *Gnai2*ako animals. Scale bar = 20 μm. *(F)* Average cell size of iWAT adipocytes after 22 weeks of CD or HFD feeding was significantly reduced when analyzed in paraffin-embedded serial sections by measuring the circumference of the adipocytes. Adipocyte size distribution in iWAT of mice fed *(G)* CD or *(H)* HFD (ctrl$_{CD}$ n = 6; *Gnai2*ako$_{HFD}$ n = 5; ctrl$_{HFD}$ n = 7; *Gnai2*ako$_{HFD}$ n = 11). Data were analyzed using multiple comparison two-way ANOVA followed by post-hoc comparison with Bonferroni's multiple comparison *(B-D, F-H)* and are presented as means ± SEMs. Statistical difference between the four treatments is indicated: *$P < 0.05$, **$P < 0.01$, ***$P < 0.001$.
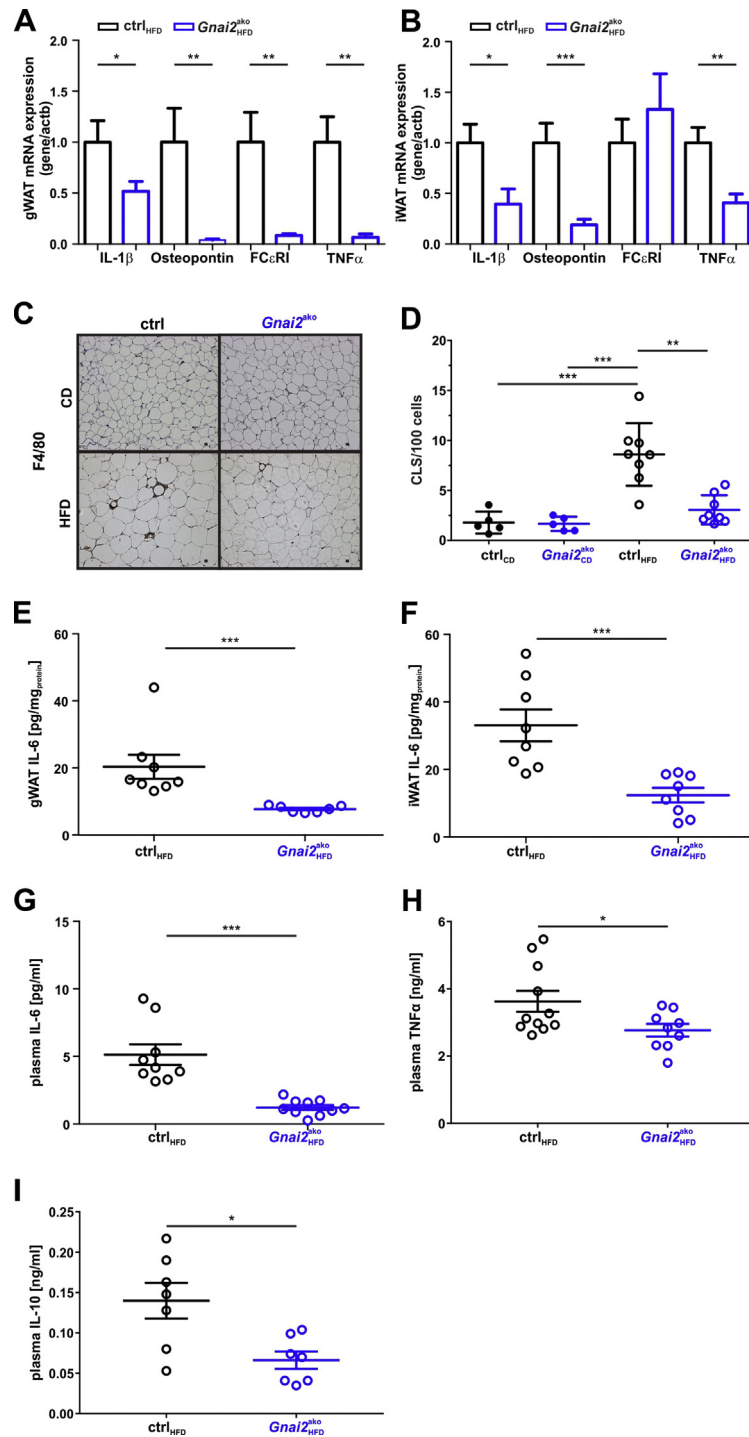
Figure 3: Decreased inflammatory parameters in HFD-fed *Gnai2*ako mice. RT-qPCR of IL-1β, osteopontin, FCεRI and TNFα in HFD-fed ctrl and *Gnai2*ako (*A*) gWAT and (*B*) iWAT. (*C*) Representative F4/80 staining of paraffin-embedded 8 μm serial sections of gWAT derived from ctrl and *Gnai2*ako mice receiving either CD (upper panel) or HFD (lower panel). (*D*) Statistical analysis of crown-like structure formation in CD- and HFD-fed ctrl and *Gnai2*ako gWAT. Significantly less CLS formation was detectable in HFD-fed *Gnai2*ako gWAT. IL-6 levels measured in (*E*) gWAT, (*F*) iWAT and (*G*) plasma were significantly lower in HFD-fed *Gnai2*ako mice compared to HFD-fed ctrl. Plasma concentrations of (*H*) TNFα and (*I*) IL-10 were significantly reduced in HFD-fed *Gnai2*ako mice. Data were analyzed using multiple comparison two-way ANOVA followed by post-hoc comparison with Bonferroni's multiple comparison (*D*) or the Student *t* test (*A, B, E-I*) and are presented as means ± SEMs. Statistical difference between the two genotypes is indicated: *$P < 0.05$, **$P < 0.01$, ***$P < 0.001$.
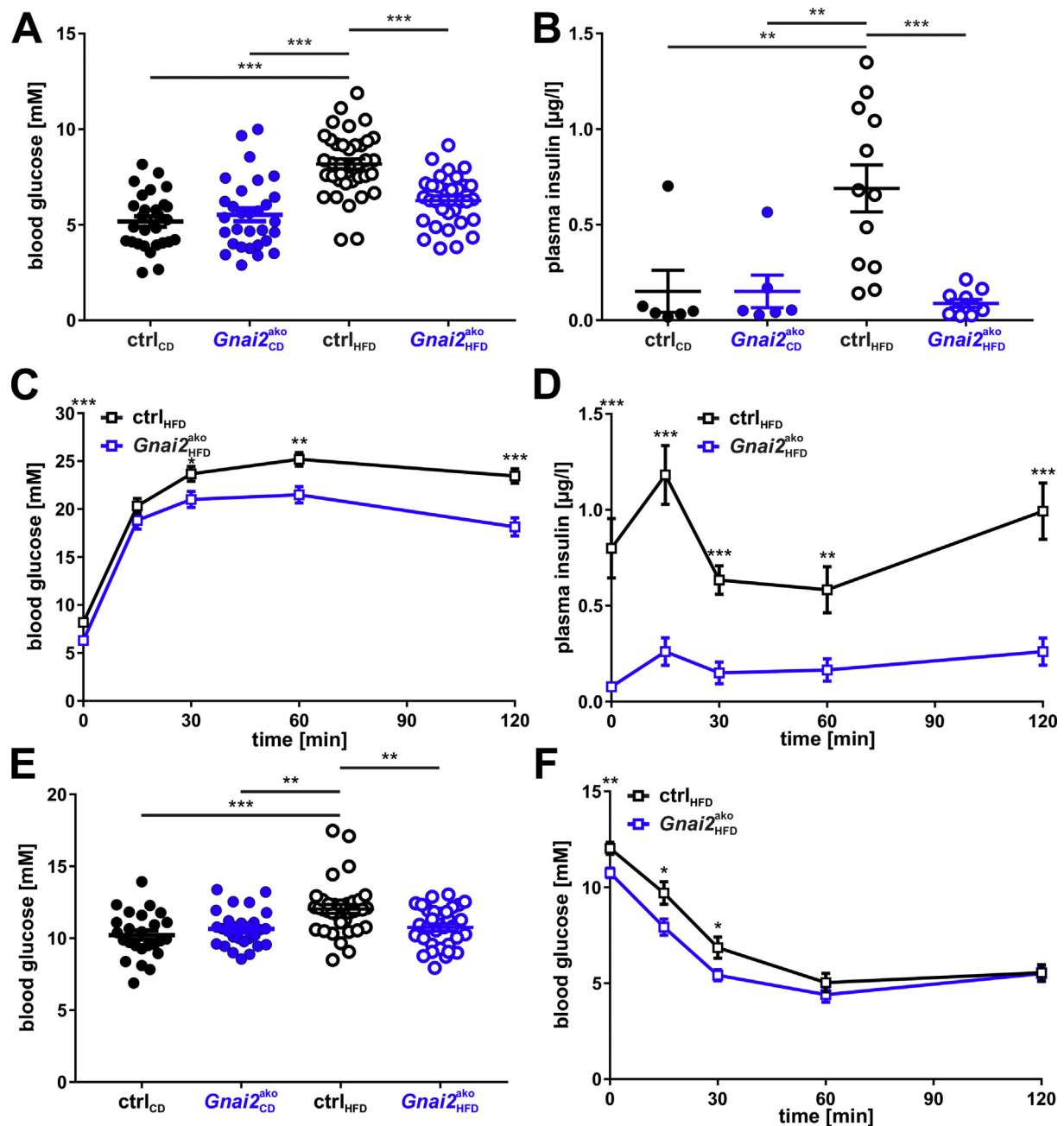
Figure 4: Improved glucose handling in HFD-fed *Gnai2*ako mice. *(A)* Basal blood glucose levels of CD- and HFD-fed ctrl and *Gnai2*ako mice. Basal blood glucose levels were significantly lower in HFD-fed *Gnai2*ako mice compared to HFD-ctrl mice. *(B)* Basal plasma insulin levels of HFD-fed *Gnai2*ako mice were significantly lower compared to HFD-fed ctrl mice but unchanged compared to CD-fed ctrl and *Gnai2*ako mice. Basal plasma insulin levels were determined after 12-h fasting prior to the glucose challenge. *(C)* Blood glucose levels of 28-week-old HFD-fed *Gnai2*ako mice were significantly lower 30, 60, and 120 min following i.p. injection of 2 mg/g body weight glucose after overnight fasting compared to HFD-fed ctrl (ctrl$_{HFD}$ n = 12; *Gnai2*ako$_{HFD}$ n = 12). *(D)* Significantly lower plasma insulin levels in HFD-fed *Gnai2*ako mice compared to ctrl animals at all indicated time points (ctrl$_{HFD}$ n = 12; *Gnai2*ako$_{HFD}$ n = 12). *(E)* Blood glucose levels measured after 4-h fasting were significantly lower in HFD-fed *Gnai2*ako compared to HFD-fed ctrl mice. *(F)* Significantly lower blood glucose levels in HFD-fed *Gnai2*ako before and after 15, 30, and 60 min following the i.p. injection of 1 mU/g body weight insulin after 4-h fasting compared to HFD-fed ctrl littermates (ctrl$_{HFD}$ n = 12; *Gnai2*ako$_{HFD}$ n = 12). Data were analyzed using multiple comparison two-way ANOVA followed by post-hoc comparison with Bonferroni's multiple comparison (A-F) are presented as means ± SEMs. Statistical difference between the two genotypes is indicated: *$P < 0.05$, **$P < 0.01$, ***$P < 0.001$.

TD-NMR findings, we measured individual weights of brown, gonadal and inguinal fat depots derived from CD- and HFD-fed *Gnai2*ako and ctrl mice at the end of the study (Figure 1K-N). In accordance with the MRI data, samples from inguinal and gonadal fat depot masses of HFD-fed *Gnai2*ako had a reduced weight compared to HFD-ctrl animals (Figure 1K, M, N). Taken together, these results demonstrate that in the

absence of adipocyte Gα$_{i2}$ lipid storage and body weight gain is reduced under excessive caloric intake.

Next, we analyzed livers of HFD-fed ctrl and *Gnai2*ako animals, which are crucial for fat metabolism (Supplemental Fig. 3). In line with the reduced body weight, individual liver weights were significantly reduced (Supplemental Fig. 3A), an effect that was mitigated when
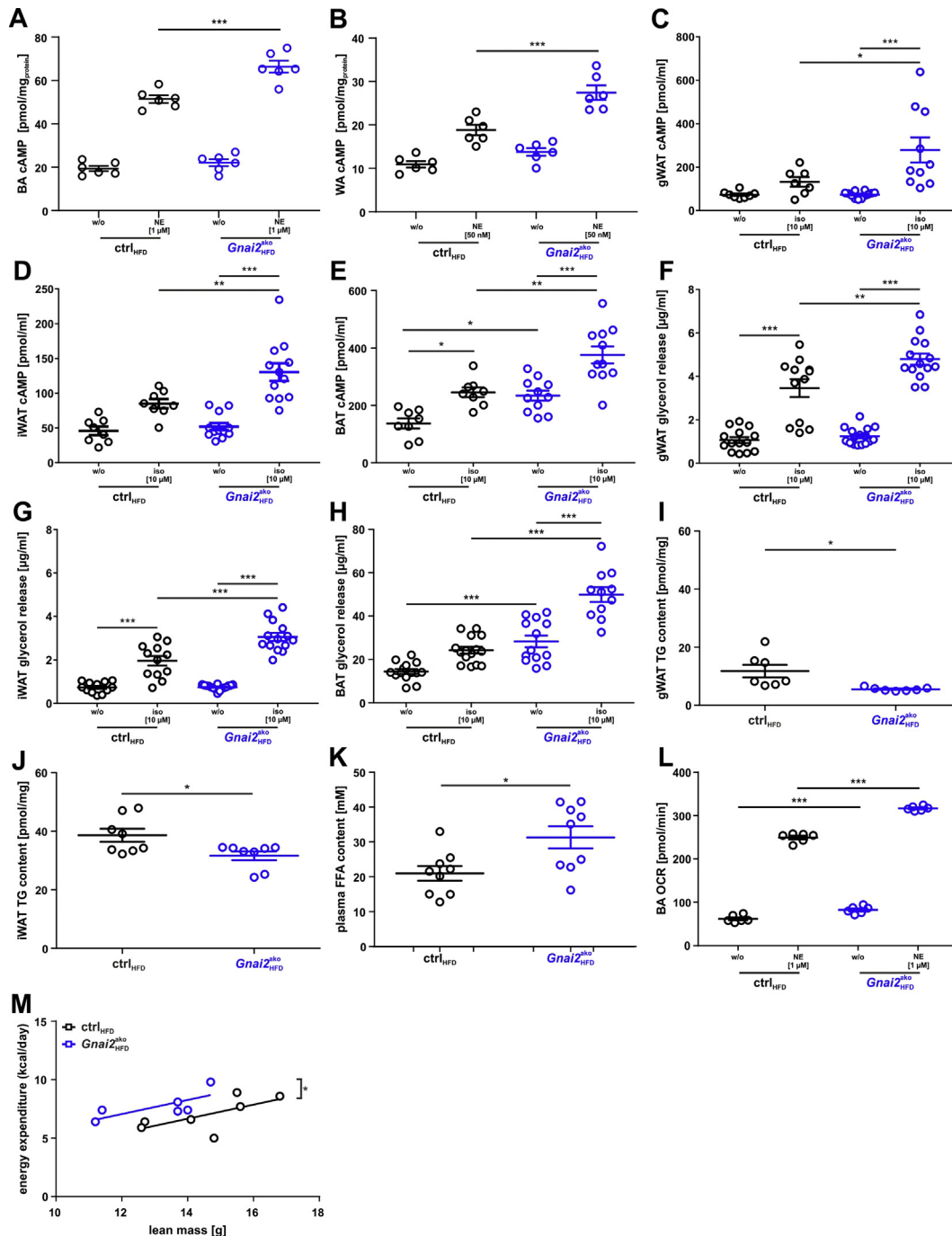
Figure 5: Increased intracellular cAMP levels and *ex vivo* lipolysis in HFD-fed *Gnai2*[ako] mice. cAMP accumulation was measured under basal and stimulated (1 μM norepinephrine (NE) in brown adipocyte primaries (BA) and 50 nM NE in WA) conditions in (*A*) BA and (*B*) WA isolated from HFD-fed ctrl and *Gnai2*[ako] mice. Adrenergic stimulation resulted in significantly higher cAMP levels of HFD *Gnai2*[ako] adipocytes compared to controls. (*C-E*) cAMP accumulation was measured under basal and stimulated (10 μM isoproterenol (iso)) conditions in (*C*) gWAT, (*D*) iWAT and (*E*) BAT of HFD-fed ctrl and *Gnai2*[ako] mice for 15 min in the presence of 1 mM IBMX. Significantly more cAMP accumulated upon adrenergic stimulation in BAT and WAT. Basal cAMP levels were significantly increased in BAT derived from *Gnai2*[ako] relative to controls. (*F-H*) Glycerol release was measured in gWAT, iWAT and BAT of HFD-fed ctrl and *Gnai2*[ako] mice. The glycerol release was significantly increased upon adrenergic stimulation in gWAT, iWAT, and BAT of HFD-fed *Gnai2*[ako] mice in comparison to ctrl animals. Basal glycerol release was significantly increased in the absence of Gα[i2] in BAT of HFD-fed *Gnai2*[ako] compared to ctrl mice. Significantly lower triglyceride levels in (*I*) gWAT and (*J*) iWAT of HFD-fed ctrl and *Gnai2*[ako] mice. (*K*) Significantly higher free fatty acid levels in the plasma of HFD-fed *Gnai2*[ako] compared to HFD-fed ctrl mice. (*L*) Oxygen consumption rate (OCR) was measured before and after the addition of 1 μM norepinephrine (NE). Basal and NE-stimulated OCR were significantly increased in brown adipocyte primaries isolated from *Gnai2*[ako] mice compared to ctrl mice. (*M*) Regression analysis of *in vivo* measured energy expenditure per day and animal *vs.* lean body mass. Significantly higher total energy expenditure in HFD-fed *Gnai2*[ako] compared to ctrl mice. Data were analyzed using multiple comparison two-way ANOVA followed by post-hoc comparison with Bonferroni's multiple comparison (*A-H, L*), the Student *t* test (*I-K*) or ANCOVA (*M*) and are presented as means ± SEMs. Statistical difference between the two genotypes is indicated: $^*P < 0.05$, $^{**}P < 0.01$, $^{***}P < 0.001$.

liver weight was normalized to the body weight (Supplemental Fig. 3B). These findings correspond to the histological assessments of the livers by H&E and Oil Red O staining that showed no differences in lipid droplet accumulation between HFD-fed ctrl and *Gnai2*[ako] mice (Supplemental Figs. 3C and D). Measuring hepatic triglyceride content as an indicator of liver steatosis revealed increased, but not significantly, triglyceride levels in HFD-fed *Gnai2*[ako] mice compared to littermate controls (Supplementary Fig. 3E).

Adipocyte size and number determine fat mass. Therefore, we measured adipocyte cell areas in different paraffin sections from gWAT and iWAT of *Gnai2*[ako] and ctrl mice. gWAT and iWAT adipocytes obtained from HFD-fed *Gnai2*[ako] mice were significantly smaller compared to HFD-fed control counterparts (Figure 2A—H). BAT morphology was similar between the two phenotypes (Supplementary Fig. 2A).

Since enlarged hypertrophic adipocytes relate to massively increased inflammation, we next tested whether the observed changes in adipocyte morphology were associated with a reduced inflammatory state in mice lacking Gα_{i2} specifically in adipocytes. Indeed, qPCR analysis showed that expression levels of FCεRI and the inflammatory cytokines IL-1β, osteopontin and TNFα were significantly reduced in gWAT and iWAT of HFD-fed *Gnai2*[ako] mice compared to controls (Figure 3A,B). We also found a significantly reduced number of crown-like structures, indicating enhanced inflammation of adipose tissue following HFD-diet in the knockout mice (Figure 3C,D). F4/80 macrophage staining in HFD-fed *Gnai2*[ako] mice was almost at the level of CD-fed *Gnai2*[ako] and ctrl mice and significantly reduced compared to HFD-fed controls. In agreement with the reduced cytokine expression levels and the reduced CLS formation, IL-6 levels in gWAT and iWAT as well as IL-6, TNFα and IL-10 plasma levels were significantly lower in HFD-fed *Gnai2*[ako] mice compared to HFD-fed control mice (Figure 3E—I). These data strengthen our assumption that adipocyte Gα_{i2} is crucial for diet-induced obesity and subsequent inflammation.

3.3. Metabolic evaluation of *Gnai2*[ako] mice

Increased fasting glucose represents an early marker for metabolic distortion and implies an important risk factor for cardiovascular diseases [22]. In addition, body fat compartments are involved in the regulation of systemic energy balance and glucose homeostasis, whereas CLS formation and inflammation are particularly associated with insulin resistance. To analyze the impact of *Gnai2*-deficiency in adipocytes on glucose handling and insulin resistance, we performed i.p. glucose tolerance tests (GTT) after overnight fasting. Twenty-six-week-old HFD-fed *Gnai2*[ako] mice already started with significantly lower basal blood glucose and plasma insulin levels compared to HFD-fed ctrl littermates (Figure 4A,B). Of note, basal blood glucose and plasma insulin levels of HFD-fed *Gnai2*[ako] mice were similar to CD-fed *Gnai2*[ako] and ctrl animals. Interestingly, during the glucose challenge blood glucose levels were significantly lower after 30, 60 and 120 min in HFD-fed *Gnai2*[ako] mice compared to HFD-fed controls, pointing to an improved glucose tolerance, since HFD-feeding of ctrl animals revealed an aggravated glucose tolerance (Figure 4C). In parallel, plasma insulin levels were significantly lower at all indicated time points (0, 15, 30, 60, and 120 min) in HFD-fed *Gnai2*[ako] *vs* ctrl animals (Figure 4B,D). To check whether the glycemic changes are causative to the lower body weight or rather a direct consequence of the target deletion, 10-week old HFD-fed control and *Gnai2*[ako] mice were subjected to a GTT, a time point before weight differences reached statistical significance (Figure 1C). Basal blood glucose levels and glucose tolerance tests were similar in young HFD-fed *Gnai2*[ako] mice compared to littermate controls arguing that the glycemic changes are causative

to the lower body weight in the knockout mice (Supplemental Figs. 4A and B).

Fitting to the improved GTT of the 26-week-old, *Gnai2*[ako] mice, the insulin sensitivity of HFD-fed *Gnai2*[ako] animals was significantly improved (Figure 4E,F). Basal blood glucose levels were significantly lower already after 4-h-fasting in HFD-fed *Gnai2*[ako] mice compared to littermate controls (Figure 4E). These lower blood glucose levels remained significant at 15, 30, and 60 min after the insulin injection in the HFD-fed *Gnai2*[ako] mice compared to ctrl littermates (Figure 4F). Interestingly, plasma non-esterified fatty acid (NEFA) levels were markedly increased whereas plasma triglycerides showed similar levels in HFD-fed *Gnai2*[ako] mice and littermate controls (Figure 4G,H). These findings indicate that Gα_{i2}-deficiency in adipocytes improves glucose tolerance and insulin sensitivity and blunts diet-induced obesity.

Adipose tissue compartments exhibit functions like an endocrine organ. They secrete a wide range of adipokines that regulate inflammation, hunger, satiety, lipid and glucose metabolism. To test whether the secretion of the adipokines resistin and leptin was affected in the absence of adipocyte Gα_{i2}, we measured their plasma levels in both CD- and HFD-fed ctrl and *Gnai2*[ako] mice after 12-h-fasting (Supplementary Figs. 4F and G). Under HFD resistin and leptin levels increased compared to the levels of animals receiving a CD. However, neither resistin nor leptin levels differed between HFD-fed ctrl and *Gnai2*[ako] mice. In contrast, mRNA expression levels of adiponectin were significantly higher in gWAT and iWAT of the knockout mice in comparison to control littermates (Supplemental Fig. 4H). Thus, higher adiponectin expression levels in combination with a leaner phenotype could point to a higher sensitivity towards the secreted adipokines in our HFD-fed *Gnai2*[ako] animals.

3.4. Adipocyte function *ex vivo*

Our findings show that the specific lack of Gα_i in adipocytes provokes a leaner phenotype by a marked reduction of fat storage upon HFD-feeding. Next, we sought to gain insight into the underlying signaling pathway. Gα_i proteins control the intracellular second-messenger cyclic AMP (cAMP) by inhibiting adenylyl cyclases [23,24]. In unstimulated primary brown and white adipocytes, BAT, gWAT and iWAT from controls, cAMP levels were low but increased upon adrenergic stimulation in a similar way (Figure 5A—E). Basal cAMP levels in HFD-fed *Gnai2*[ako] brown and white adipocytes, gWAT and iWAT were similar to those of HFD-fed controls. In contrast, cAMP levels of *Gnai2*[ako] BAT were significantly higher compared to controls. Adrenergic stimulation resulted in a stronger increase of intracellular cAMP concentrations in all tissues analyzed of HFD-fed *Gnai2*[ako] mice compared to their littermate controls (Figure 5A—E). Stimulation of adenylyl cyclase *via* Gα_s increases lipolysis whereas Gα_i-driven pathways inhibit adenylyl cyclase and reduce lipolysis in adipocytes. Thus, differences in intracellular cAMP levels should affect lipolysis rates in BAT and WAT of *Gnai2*[ako] mice. As a consequence, release of non-esterified fatty acids and glycerol from the adipocytes should depend on cAMP levels. Therefore we measured glycerol release from gWAT, iWAT and BAT as an index of lipolysis. Indeed, basal lipolytic rates were significantly higher in BAT and upon adrenergic stimulation in BAT and WAT (Figure 5F—H). Although plasma triglycerides were similar in HFD-fed *Gnai2*[ako] mice and littermate controls, total triglyceride levels were significantly lower in gWAT and iWAT of HFD-fed *Gnai2*[ako] mice compared to their HFD-fed littermate controls, whereas (Figure 5I,J, Supplementary Fig. 5E). In line with this, fasting plasma NEFA levels were significantly increased in the knockout mice (Figure 5K). Taken together, *Gnai2*-deficiency restricted to adipocytes enhances intracellular cAMP concentrations upon adrenergic stimulation. As a

consequence, stored triglycerides are extensively hydrolyzed, which is reflected in increased plasma NEFA levels.

Measuring mitochondrial oxygen consumption rate (OCR) assesses the fuel metabolism and energy expenditure of primary white and brown adipocytes. Therefore we performed a seahorse assay to determine OCR of primary white and brown adipocytes. ATP-linked respiration, maximal respiratory capacity and non-mitochondrial respiration were not affected by the lack of $G\alpha_{i2}$ in brown and white adipocytes (Supplementary Fig. 6 A, B). For primary white adipocytes derived from HFD-fed $Gnai2^{ako}$ mice, an increased oxygen consumption rate with or without adrenergic-stimulation was not detectable when compared to littermate controls (Supplementary Fig. 6C). In contrast, brown adipocytes showed increased oxygen consumption rates in the absence and presence of adrenergic stimulation (Figure 5L). Of note, total energy expenditure was significantly increased in HFD-fed $Gnai2^{ako}$ compared to ctrl mice (Figure 5M). Thus lack of the $G\alpha_{i2}$-isoform in brown and white adipocytes leads to an increased energy expenditure on HFD and impedes diet-induced obesity.

Taken together, these findings suggest that upon excessive caloric intake, adipocyte $G\alpha_{i2}$ signaling contributes to an excessive accumulation of fat mass by inhibiting adipocyte lipolysis in brown and white adipocytes in a cAMP-dependent manner, decreasing total energy expenditure and enhancing lipid accumulation.

4. DISCUSSION

The present study examined the function of adipocyte $G\alpha_{i2}$ in fat cell biology and its role for the metabolic state of mice under different nutritional conditions. Mice lacking the ubiquitously expressed $G\alpha_{i2}$ protein specifically in adipocytes were studied in comparison to littermate controls. $G\alpha_{i2}$-deficiency in adipocytes results in mitigated diet-induced obesity with reduced total fat masses, smaller white adipocytes, and increased total energy expenditure that was not due to differences in food consumption or physical activity. Concomitantly, improved glucose handling and reduced inflammation of white adipose tissue became evident. Mechanistically, we observed increased cAMP levels and lipolysis upon adrenergic stimulation in brown and white adipose tissue and primary adipocytes of obese mice, accompanied by higher oxygen consumption rates of brown adipocytes resulting in increased total energy expenditure of the HFD-fed knockout mice. Overall, adipose tissue-specific deletion of $Gnai2$ decreased weight gain on diet-induced obesity. Our data indicate that $G\alpha_{i2}$ in adipocytes promotes obesity that in turn leads to local inflammation and to systemic glucose intolerance. Therefore we speculate that fat-cell $G\alpha_{i2}$ is a pivotal player in the development and aggravation of diet-induced obesity that also causes derailed metabolic alterations, such as diabetes. Our hypothesis is based on several considerations detailed below.

Visceral fat and infiltrating macrophages secrete a number of mediators, which play a role in the development of insulin resistance. Among the latter are leptin, resistin, IL-6 and tumor necrosis factor-α (TNF-α) [25—28]. Whereas plasma leptin and resistin levels were similar in our adipocyte-specific $Gnai2$-deficient mice compared to littermate controls, plasma levels of IL-6 and TNFα were significantly decreased. Consistent with this, less crown-like structures were formed in the gWAT of $Gnai2^{ako}$ mice. Crown-like structures (CLS) are formed around dying adipocytes, an area that is infiltrated by macrophages, which secrete IL-6 and TNFα. High TNFα levels correlate positively with insulin resistance [29]. Indeed, our adipocyte-specific $Gnai2$-deficient mice had improved insulin sensitivity: with lower plasma insulin levels (basal and during glucose challenge) they removed the glucose with higher efficiency from the blood compared to HFD-fed controls. Thus $Gnai2$-deficieny prevents diet-induced inflammation and development of insulin resistance.

The deletion of $Gnai2$ in brown and white adipocytes decreased weight gain on diet-induced obesity. Our data suggest a cellular mechanism responsible for the smaller adipocytes and the leaner phenotype in adipocyte-specific $Gnai2$-deficient mice. $Gnai2$-deficiency produces increased cAMP levels upon adrenergic stimulation indicating a more efficient $G\alpha_s$-mediated signaling. Consequently, lipolysis is enhanced with less triglycerides being stored in the adipocytes and thus less fat accumulation. Our results strengthen the relevance of cAMP signaling for the regulation of lipid metabolism. It has to be clarified whether impaired $G\alpha_{i2}$ coupling directly to β-adrenoceptors (β_{1-3}-AR) [30,31] or disturbed signal transduction from a specifically $G\alpha_{i2}$-coupled receptor fails to reduce $G\alpha_s$-mediated signaling in our mouse model thereby increasing total energy expenditure. A variety of $G\alpha_i$-coupled receptors has been described to act in an autocrine inhibitory fashion on white adipocytes, e.g. lactate, nicotinic acid [32—35]. In line with our findings, it has recently been published that acute stimulation of G_s-coupled receptors specifically in adipocytes increases ex vivo lipolysis and plasma NEFA levels inducing hypoglycemia [36]. These results underline our hypothesis that deletion of $G\alpha_{i2}$ enhances $G\alpha_s$-signaling in adipocytes. A different approach to study how $G\alpha_{i2}$ affects obesity and metabolism was shown in a study using a knockin mouse line in which regulator of G-protein signaling-insensitive $G\alpha_{i2}$ (G184S) was expressed [37]. These authors find a comparable phenotype to our adipocyte-specific $G\alpha_{i2}$ deficiency model. However, one has to be cautious with the interpretation of these data, since the mutant is ubiquitously expressed and the mice have a complex and severe phenotype, e.g. these mice already start with significantly lower body weights due to growth retardation [38]. Our mouse model lacks the $G\alpha_{i2}$ protein specifically in adipocytes and the mutant mice do not reveal any growth or body weight differences before onset of the HFD. In addition, several PTX-based approaches have shown the impact of $G\alpha_i$ proteins on inhibition of intracellular cAMP levels and lipolysis [32,39].

The presented data indicate the importance and relevance of identifying $G\alpha_{i2}$—specific functions in metabolically active tissues. $G\alpha_{i2}$ proteins are pertussis toxin sensitive and were supposed to inhibit insulin secretion. Previously, we deleted $Gnai2$ specifically in β—cells [9], which had a negative effect on glucose handling and insulin sensitivity. In contrast to the beneficial effects of β-cell $G\alpha_{i2}$ on insulin secretion and glucose handling, fat cell $G\alpha_{i2}$ aggravates body weight gain, inflammation, fat storage, insulin resistance, and energy expenditure under high caloric intake.

5. CONCLUSIONS

Collectively, our findings expand knowledge of the physiological functions of the adipocyte $G\alpha_{i2}$ isoform in obesity and suggest inhibition of $G\alpha_{i2}$-dependent signaling pathways as a potential target to intervene in the development of excessive weight gain, obesity-induced inflammation, and insulin resistance. Furthermore, this work underlines the importance of understanding the metabolic roles of the predominantly expressed $G\alpha_{i2}$ isoform in relevant insulin-dependent tissues, and to dissect $G\alpha_{i1-3}$ isoform-specific functions in these tissues for future therapeutic strategies.

FUNDING

Original Article

CONFLICT OF INTEREST

None declared.

APPENDIX A. SUPPLEMENTARY DATA

Supplementary data to this article can be found online at https://doi.org/10.1016/j.molmet.2020.101029.

REFERENCES

[1] Czech, M.P., Richardson, D.K., Smith, C.J., 1977. Biochemical basis of fat cell insulin resistance in obese rodents and man. Metabolism 26(9):1057—1078.

[2] Hotamisligil, G.S., 2006. Inflammation and metabolic disorders. Nature 444(7121):860—867.

[3] Olefsky, J.M., Glass, C.K., 2010. Macrophages, inflammation, and insulin resistance. Annual Review of Physiology 72:219—246.

[4] Weisberg, S.P., McCann, D., Desai, M., Rosenbaum, M., Leibel, R.L., Ferrante Jr., A.W., 2003. Obesity is associated with macrophage accumulation in adipose tissue. Journal of Clinical Investigation 112(12):1796—1808.

[5] Hilger, D., Masureel, M., Kobilka, B.K., 2018. Structure and dynamics of GPCR signaling complexes. Nature Structural & Molecular Biology 25(1):4—12.

[6] Wong, Y.H., Federman, A., Pace, A.M., Zachary, I., Evans, T., Pouyssegur, J., et al., 1991. Mutant alpha subunits of Gi2 inhibit cyclic AMP accumulation. Nature 351(6321):63—65.

[7] Beer-Hammer, S., Lee, S.C., Mauriac, S.A., Leiss, V., Groh, I.A.M., Novakovic, A., et al., 2018. Gαi proteins are indispensable for hearing. Cellular Physiology and Biochemistry 47(4):1509—1532.

[8] Köhler, D., Devanathan, V., Bernardo de Oliveira Franz, C., Eldh, T., Novakovic, A., Roth, J.M., et al., 2014. Gαi2- and Gαi3-deficient mice display opposite severity of myocardial ischemia reperfusion injury. PLoS One 9(5): e98325.

[9] Leiss, V., Flockerzie, K., Novakovic, A., Rath, M., Schönsiegel, A., Birnbaumer, L., et al., 2014. Insulin secretion stimulated by arginine and its metabolite ornithine depends on Gαi2. American Journal of Physiology. Endocrinology and Metabolism.

[10] Minetti, G.C., Feige, J.N., Bombard, F., Heier, A., Morvan, F., Nurnberg, B., et al., 2014. Galphai2 signaling is required for skeletal muscle growth, regeneration, and satellite cell proliferation and differentiation. Molecular and Cellular Biology 34(4):619—630.

[11] Gohla, A., Klement, K., Piekorz, R.P., Pexa, K., vom Dahl, S., Spicher, K., et al., 2007. An obligatory requirement for the heterotrimeric G protein G$_{i3}$ in the antiautophagic action of insulin in the liver. Proceedings of the National Academy of Sciences of the United States of America 104(8): 3003—3008.

[12] Wiege, K., Ali, S.R., Gewecke, B., Novakovic, A., Konrad, F.M., Pexa, K., et al., 2013. Gα$_{i2}$ is the essential Gα$_i$ protein in immune complex-induced lung disease. The Journal of Immunology 190(1):324—333.

[13] Wiege, K., Le, D.D., Syed, S.N., Ali, S.R., Novakovic, A., Beer-Hammer, S., et al., 2012. Defective macrophage migration in Gα$_{i2}$- but not Gα$_{i3}$-deficient mice. The Journal of Immunology 189(2):980—987.

[14] Rudolph, U., Finegold, M.J., Rich, S.S., Harriman, G.R., Srinivasan, Y., Brabet, P., et al., 1995. Ulcerative colitis and adenocarcinoma of the colon in Gα$_{i2}$-deficient mice. Nature Genetics 10(2):143—150.

[15] Sassmann, A., Offermanns, S., Wettschureck, N., 2010. Tamoxifen-inducible Cre-mediated recombination in adipocytes. Genesis 48(10):618—625.

[16] Illison, J., Tian, L., McClafferty, H., Werno, M., Chamberlain, L.H., Leiss, V., et al., 2016. Obesogenic and diabetogenic effects of high-calorie nutrition require adipocyte BK channels. Diabetes 65(12):3621—3635.

[17] Machann, J., Thamer, C., Schnoedt, B., Haap, M., Haring, H.U., Claussen, C.D., et al., 2005. Standardized assessment of whole body adipose tissue topography by MRI. Journal of Magnetic Resonance Imaging 21(4):455—462.

[18] Sartorius, T., Ketterer, C., Kullmann, S., Balzer, M., Rotermund, C., Binder, S., et al., 2012. Monounsaturated fatty acids prevent the aversive effects of obesity on locomotion, brain activity, and sleep behavior. Diabetes 61(7): 1669—1679.

[19] Gohla, A., Klement, K., Nurnberg, B., 2007. The heterotrimeric G protein G$_{i3}$ regulates hepatic autophagy downstream of the insulin receptor. Autophagy 3(4):393—395.

[20] Leopoldt, D., Harteneck, C., Nurnberg, B., 1997. G proteins endogenously expressed in Sf 9 cells: interactions with mammalian histamine receptors. Naunyn-Schmiedeberg's Archives of Pharmacology 356(2):216—224.

[21] Plummer, N.W., Spicher, K., Malphurs, J., Akiyama, H., Abramowitz, J., Nürnberg, B., et al., 2012. Development of the mammalian axial skeleton requires signaling through the Gα$_i$ subfamily of heterotrimeric G proteins. Proceedings of the National Academy of Sciences of the United States of America 109(52):21366—21371.

[22] Shaye, K., Amir, T., Shlomo, S., Yechezkel, S., 2012. Fasting glucose levels within the high normal range predict cardiovascular outcome. American Heart Journal 164(1):111—116.

[23] Birnbaumer, L., 1990. G proteins in signal transduction. Annual Review of Pharmacology and Toxicology 30:675—705.

[24] Gilman, A.G., 1987. G proteins: transducers of receptor-generated signals. Annual Review of Biochemistry 56:615—649.

[25] Kershaw, E.E., Flier, J.S., 2004. Adipose tissue as an endocrine organ. Journal of Clinical Endocrinology & Metabolism 89(6):2548—2556.

[26] Murano, I., Barbatelli, G., Parisani, V., Latini, C., Muzzonigro, G., Castellucci, M., et al., 2008. Dead adipocytes, detected as crown-like structures, are prevalent in visceral fat depots of genetically obese mice. The Journal of Lipid Research 49(7):1562—1568.

[27] Cortez, M., Carmo, L.S., Rogero, M.M., Borelli, P., Fock, R.A., 2013. A high-fat diet increases IL-1, IL-6, and TNF-alpha production by increasing NF-kappaB and attenuating PPAR-gamma expression in bone marrow mesenchymal stem cells. Inflammation 36(2):379—386.

[28] Mauer, J., Denson, J.L., Bruning, J.C., 2015. Versatile functions for IL-6 in metabolism and cancer. Trends in Immunology 36(2):92—101.

[29] Hotamisligil, G.S., Shargill, N.S., Spiegelman, B.M., 1993. Adipose expression of tumor necrosis factor-alpha: direct role in obesity-linked insulin resistance. Science 259(5091):87—91.

[30] Lafontan, M., Berlan, M., 1993. Fat cell adrenergic receptors and the control of white and brown fat cell function. The Journal of Lipid Research 34(7):1057—1091.

[31] Martin, N.P., Whalen, E.J., Zamah, M.A., Pierce, K.L., Lefkowitz, R.J., 2004. PKA-mediated phosphorylation of the beta1-adrenergic receptor promotes Gs/Gi switching. Cellular Signalling 16(12):1397—1403.

[32] Ahmed, K., Tunaru, S., Tang, C., Muller, M., Gille, A., Sassmann, A., et al., 2010. An autocrine lactate loop mediates insulin-dependent inhibition of lipolysis through GPR81. Cell Metabolism 11(4):311—319.

[33] Plaisance, E.P., Lukasova, M., Offermanns, S., Zhang, Y., Cao, G., Judd, R.L., 2009. Niacin stimulates adiponectin secretion through the GPR109A receptor. American Journal of Physiology. Endocrinology and Metabolism 296(3):E549—E558.

[34] Taggart, A.K., Kero, J., Gan, X., Cai, T.Q., Cheng, K., Ippolito, M., et al., 2005. (D)-beta-Hydroxybutyrate inhibits adipocyte lipolysis via the nicotinic acid receptor PUMA-G. Journal of Biological Chemistry 280(29): 26649—26652.

[35] Cai, T.Q., Ren, N., Jin, L., Cheng, K., Kash, S., Chen, R., et al., 2008. Role of GPR81 in lactate-mediated reduction of adipose lipolysis. Biochemical and Biophysical Research Communications 377(3):987—991.

[36] Caron, A., Reynolds, R.P., Castorena, C.M., Michael, N.J., Lee, C.E., Lee, S., et al., 2019. Adipocyte Gs but not Gi signaling regulates whole-body glucose homeostasis. Molecular metabolism 27:11—21.

[37] Huang, X., Charbeneau, R.A., Fu, Y., Kaur, K., Gerin, I., MacDougald, O.A., et al., 2008. Resistance to diet-induced obesity and improved insulin sensitivity in mice with a regulator of G protein signaling-insensitive G184S Gnai2 allele. Diabetes 57(1):77—85.

[38] Huang, X., Fu, Y., Charbeneau, R.A., Saunders, T.L., Taylor, D.K., Hankenson, K.D., et al., 2006. Pleiotropic phenotype of a genomic knock-in of an RGS-insensitive G184S Gnai2 allele. Molecular and Cellular Biology 26(18): 6870—6879.

[39] Mangmool, S., Kurose, H., 2011. G(i/o) protein-dependent and -independent actions of Pertussis Toxin (PTX). Toxins 3(7):884—899.